Waveguide mode amplitude estimation using warping and phase compensation

Julien BonnelSalvatore CaporaleAaron Thode

Citation: The Journal of the Acoustical Society of America **141**, 2243 (2017); doi: 10.1121/1.4979057
View online: http://dx.doi.org/10.1121/1.4979057
View Table of Contents: http://asa.scitation.org/toc/jas/141/3
Published by the Acoustical Society of America

Waveguide mode amplitude estimation using warping and phase compensation

Julien Bonnel[a)]
École Nationale Supérieure de Techniques Avancées de Bretagne, Lab-STICC (UMR CNRS 6285), 2 rue Francois Verny, 29806 Brest Cedex 9, France

Salvatore Caporale
Institute of Sensors, Signals and Systems, Heriot-Watt University, Edinburgh, Scotland, United Kingdom

Aaron Thode
Marine Physical Laboratory, Scripps Institution of Oceanography, University of California San Diego, La Jolla, California 92093, USA

(Received 14 December 2016; revised 3 March 2017; accepted 10 March 2017; published online 31 March 2017)

In shallow water, low-frequency propagation can be described by modal theory. Acoustical oceanographic measurements under this situation have traditionally relied on spatially filtering signals with arrays of synchronized hydrophones. Recent work has demonstrated how a method called warping allows isolation of individual mode arrivals on a single hydrophone, a discovery that subsequently opened the door for practical single-receiver source localization and geoacoustic inversion applications. Warping is a non-linear resampling of the signal based on a simplistic waveguide model. Because warping is robust to environmental mismatch, it provides accurate estimates of the mode phase even when the environment is poorly known. However, the approach has issues with mode amplitude estimation, particularly for the first arriving mode. As warping is not invariant to time shifting, it relies on accurate estimates of the signal's time origin, which in turn heavily impacts the first mode's amplitude estimate. Here, a revised warping operator is proposed that incorporates as much prior environmental information as possible, and is actually equivalent to compensating the relative phase of each mode. Warping and phase compensation are applied to both simulated and experimental data. The proposed methods notably improve the amplitude estimates of the first arriving mode.
[http://dx.doi.org/10.1121/1.4979057]

[ZHM] Pages: 2243–2255

I. INTRODUCTION

In shallow water and littoral environments, sound propagation is greatly influenced by both the source location and environmental properties. Estimating these properties *in situ* using ocean acoustics is an active research field, and various inversion methods have been developed. Most existing methods stem from Matched Field Processing (MFP),[1] a conceptual extension of conventional array processing that compares the recorded acoustic field against simulated replicas generated at multiple candidate positions. Another important goal is infering the uncertainty associated with source/environmental estimations, and a variety of approaches have been explored, including using Bayesian methodology (e.g., Refs. 2–4). Obviously, one wants to estimate source/environment parameters with small uncertainties, thus adaptive signal processing methods have been developed to extract relevant information from the acoustic data, to be used as inputs for adaptive inverse algorithms (e.g., Ref. 5). A specific example of this approach is Matched Mode Processing (MMP),[6] where the inverse problem is separated into two consecutive steps. First, spatial modal filtering is applied on the acoustic data to decompose the acoustic field into a series of propagating modes, traditionally using a vertical array. Then these filtered modes are compared to simulated replicas. The modal filtering step is thus crucial when applying MMP techniques. This article focuses on modal filtering for low-frequency ($f < 250$ Hz) impulsive sources in shallow water ($D < 200$ m) waveguides using a single hydrophone, with particular emphasis on recovering the correct modal amplitudes at relatively close ranges ($1 < r < 10$ km), a situation where the modal arrivals overlap in time. The topic presented here has a broad spectrum of applications, including single-receiver marine mammal localization and geoacoustic inversion. In particular accurate extraction of modal amplitudes is of paramount importance when inferring source depth, and/or seabed attenuation. The fact the method is restricted to impulsive sources prevents its application on ambient noise. However, it can be applied to both man-made sources (e.g., airgun, explosion) or baleen whale vocalizations (e.g., "gunshot" sound produced by bowhead and right whales).

At the frequencies and water depths discussed here, the oceanic environment acts as a dispersive waveguide, and propagation can be described by normal-mode theory.[7] The acoustic field can be modeled as a small set of modes that

[a)]Electronic mail: julien.bonnel@ensta-bretagne.fr

propagate dispersively, with each frequency component traveling with its own group speed. As stated above, if individual modes can be adequately isolated from the received signal, then the information carried by each mode can be used for localization and inversion. Modal filtering is traditionally performed by spatially filtering signals on vertical line array (VLA) of synchronized receivers, exploiting the orthogonal relationship between modes in the vertical dimension.[8,9] However, the success of this approach requires a reasonably accurate ocean model to generate modal weighting functions, as well as an array that spans a significant fraction of the ocean column. For the multitude of ocean datasets that consist of a single hydrophone and/or sparse networks of non-synchronized instruments (classically used to monitor ambient noise and/or marine mammals), it is impossible to resort to spatial filtering. However, it is possible to replace the spatial diversity provided by an array with frequency diversity, as provided by a broadband source. This allowed successful Matched Impulse Response localization (e.g., Ref. 10) and geoacoustic inversion (e.g., Ref. 11). However, such methods do not benefit from physical inputs as can be obtained through modal decomposition, and they usually have experimental constraints (such as the need to use several snapshots[10]) and/or require *a priori* information (such as knowing the experimental geometry and/or the source waveform[11]). It is nonetheless possible to filter modes with a single hydrophone and a single snapshot, without information on the experimental geometry. At large enough ranges, modes are naturally separated in time, and/or in the time/frequency domain (e.g., Ref. 12). However, at closer ranges, dedicated processing is required for mode separation. It has been recently shown that modal filtering can be achieved by combining time-frequency (TF) analysis and a nonlinear resampling method called *warping*.[13,14] Such resampling is performed using a mathematical *warping function*, which usually derives from a simple environmental propagation model. The warping function that is (nearly) unanimously used in the ocean acoustics community derives from an ideal-isovelocity waveguide approximation.[14–25] The utility of such a model is that it provides a simple analytical warping solution that is applicable to every mode present in the signal. Other approximations exist that also permit warping every mode at once, e.g., approximated Pekeris waveguide,[13] waveguide invariant[26,27] or beam-displacement ray-mode theory.[28] However, these approaches have not been used nearly as extensively as the warping derived from the ideal-isovelocity waveguide approximation.

Warping based on the ideal-isovelocity approximation, called "isovelocity warping" here, has been found to be robust to environmental mismatch, allowing successful modal filtering for real data in relatively complex shallow-water environments. It has been used by various researchers for numerous applications, including geoacoustic inversion,[15–17] water column tomography,[18] marine mammal localization,[19–21] etc. Nonetheless, modal filtering using isovelocity warping presents some limitations. Filtered modes are by nature complex numbers. Modal filtering using isovelocity warping provides a reliable estimate of the mode phase; however, it seems to be less reliable for mode amplitude estimation, in particular, the first arriving mode. Indeed, for all the successful applications of warping previously cited,[14–21] the inversion algorithm was based on the modal phase (or, equivalently, on the modal TF dispersion curves that directly derives from the modal phase). On the other hand, very few at-sea applications have benefited from mode amplitude estimated using warping.[22–25] Single receiver MMP—which should be straightforward after warping—has found a few source localization applications.[24,25] As far as we know, single receiver MMP has never been applied successfully to geoacoustic inversion, which requires accurate reconstruction of both mode phase and amplitude. The mode amplitude estimation problem seems particularly problematic for mode 1, as can be seen on Figs. 7 and 9 and 11 in Ref. 14 or Fig. 8 in Ref. 23. A good estimation of the mode 1 amplitude is particularly crucial for applications where as few as 2 or 3 modes are propagating.[19,20]

This paper revisits modal filtering using isovelocity warping, and shows how modal amplitude estimation highly depends on the correct choice of time origin. In an ideal-isovelocity waveguide, the time origin is naturally defined as the source emission time. In a more complex environment, the warping time origin has no clear definition and must be chosen arbitrarily. Here we first demonstrate how careful selection of the time origin greatly improves modal amplitude estimation performance, particularly for the first arriving mode. We then present new solutions for filtering modes, by changing the warping function to incorporate more detailed environmental information, if that information is previously known. This "environment-specific" warping allows a perfect transform of one mode, but requires a different warping function to extract another mode from the same signal. Such an approach has previously been developed for ultrasonic guided waves,[29,30] but has not been applied previously to underwater acoustics. We show that this alternative warping approach yields results very similar to processing based on phase compensation, which has also been considered to characterize ultrasonic guided waves[31] but never applied as a modal filtering method in ocean acoustics.

The remainder of the paper is organized as follows. Section II briefly recalls the basis of modal propagation and warping theory. Section III presents the principles of dispersion-based processing: environment-specific warping and phase compensation. These techniques are then applied on simulated data in Sec. IV, and are then used to extract mode amplitudes from the Shallow Water 2006 Experiment in Sec. V.

II. MODAL PROPAGATION AND WARPING THEORY

A. Modal propagation

In shallow water ($D < 200$ m), low-frequency ($f < 250$ Hz) acoustic propagation is conveniently described using normal-mode theory. Given a broadband source emitting at depth z_s in a range-independent waveguide, the spectral component of the pressure field $y(f)$ received at depth z_r after propagation over a range r is given by[7]

$$y(f) \approx QS(f) \sum_{m=1}^{N} \Psi_m(f, z_s) \Psi_m(f, z_r) \frac{e^{(jrk_m(f) - r\beta_m(f))}}{\sqrt{k_m(f) r}}, \tag{1}$$

where N is the number of propagating modes, and $k_m(f)$, $\beta_m(f)$ and Ψ_m are, respectively, the real part of the horizontal wave number, the imaginary part of the horizontal wave number, and the modal depth function of mode m at frequency f. The term $S(f)$ is the source spectrum, and $Q = (e^{j\pi/4})/(\sqrt{8\pi}\rho(z_s))$ represents a constant factor with $\rho(z_s)$ as the water density at the source depth z_s. If the source is perfectly impulsive, then $S(f) = e^{j2\pi f t_s}$ with t_s being the source emission time. Equation (1) can be written in a more compactly as

$$y(f) = \sum_{m=1}^{N} A_m(f) e^{j\phi_m(f)}, \tag{2}$$

where

$$A_m(f) = Q \frac{\Psi_m(f, z_s) \Psi_m(f, z_r)}{\sqrt{k_m(f) r}} e^{-r\beta_m(f)} \tag{3}$$

is the modal amplitude and

$$\phi_m(f) = k_m(f) r + 2\pi f t_s \tag{4}$$

is the mode phase. One can note how the mode amplitude $A_m(f)$ depends on $\beta_m(f)$, which in turns depends on the seabed attenuation.

When observing the received signal, the TF position of a given mode is defined here as the *dispersion curve*. It is given by

$$\tau_m(f) = \frac{1}{2\pi} \frac{d}{df} [\phi_m(f)] \tag{5a}$$

$$= t_s + \frac{r}{v_{gm}(f)}, \tag{5b}$$

where $v_{gm}(f) = 2\pi(df/dk_m)$ is the group speed of mode m.

B. Warping theory

Let us consider a signal $y(x) = a(x) e^{j2\pi x_0 \Phi(x)}$ where x can represent either time or frequency, and x_0 is a constant. By definition, warping operates on $y(x)$ according to

$$\mathbf{W}y(x) = \sqrt{|h'(x)|}\, y[h(x)], \tag{6}$$

where $\mathbf{W}y(x)$ is the warped signal, and $h(x)$ is a warping function, with $h'(x)$ its derivative with respect to x. An important constraint is that the warping function $h(x)$ must be bijective, and thus warping is an invertible transformation. Any warped signal can be unwarped using $h^{-1}(x)$ as the new warping function. Practically, warping is implemented by resampling (interpolating) $y(x)$ with a new variable $x_2 = h(x)$. Note that the orthogonalization factor $\sqrt{|h'(x)|}$ ensures energy conservation between $\mathbf{W}y$ and y. It also makes the warping operator unitary, such that orthogonal projections applied in the warped domain are orthogonal to the unwarped domain as well.[32]

The objective of warping is to linearize $\Phi(x)$, the phase of $y(x)$. Warping is adapted if $h(x) = \Phi^{-1}(x)$. In this case, if y is a time domain signal so that $y(t) = a(t) e^{j2\pi f_0 \Phi(t)}$, then the warping function is $h(t) = \Phi^{-1}(t)$ and the warped signal $\mathbf{W}y(t) = b(t) e^{j2\pi f_0 t}$ becomes a continuous tone of frequency f_0 modulated by $b(t) = \sqrt{|h'(t)|}\, a[h(t)]$. If y is a frequency domain signal $y(f) = a(f) e^{j2\pi t_0 \Phi(f)}$, then the warping function is $h(f) = \Phi^{-1}(f)$ and the warped signal $\mathbf{W}y(f) = c(f) e^{j2\pi t_0 f}$ becomes a dirac delta function at time t_0 modulated by $c(f) = \sqrt{|h'(f)|}\, a[h(f)]$. A warping that operates in the frequency domain is defined here as a frequency-warping (although the warped signal is an impulse, i.e., a Dirac in the time-domain). A warping that operates in the time domain is defined here as a time-warping (although the warped signal is a continuous tone, i.e., a Dirac function in the frequency domain).

As an example, Fig. 1 illustrates the time and frequency warping principles for three different signals. Time and/or frequency warping can be chosen, depending on the signal's TF distribution (i.e., dispersion curve). If, at any given instant, only one frequency exists, then the signal can be studied with time-warping (e.g., signal 1 on Fig. 1), and the TF shape of the warped signal becomes that of a continuous tone. On the other hand, if any given frequency corresponds with just a single time, then the signal can be studied with frequency-warping (e.g., signal 3 on Fig. 1), and the TF shape of the warped signal becomes a Dirac function. Last but not least, if the dispersion curve is bijective, then the signal can be studied with either time or frequency warping (e.g., signal 2 on Fig. 1).

III. DISPERSION-BASED PROCESSING

Warping can be adapted to any physical situation by choosing a suitable warping function h. Here dispersion-based warping requires that h is chosen such that at least one mode is transformed into a frequency-modulated impulse (frequency warping) or amplitude-modulated tone (time warping). A physical model of the environment is required so that the modal phase ϕ_m is known, which permits the warping function to be defined as $h \propto \phi_m^{-1}$. Note that as stated in Sec. II B, both h and ϕ_m may be defined in the time or frequency domain. Several useful warping functions have previously been used in the literature, and some of them are detailed below. However, it is interesting to note first that modal propagation is conveniently defined in the frequency domain through Eq. (1). As a result, a simple waveguide approximation usually leads to closed-form expressions of $\phi_m(f)$, and thus to frequency warping operators. On the other hand, time warping operators are usually obtained through a stationary phase approximation of Eq. (1), leading to an expression for $\phi_m(t)$ that is generally quite accurate, as the stationary phase approximation is reasonable for underwater acoustic normal mode propagation.

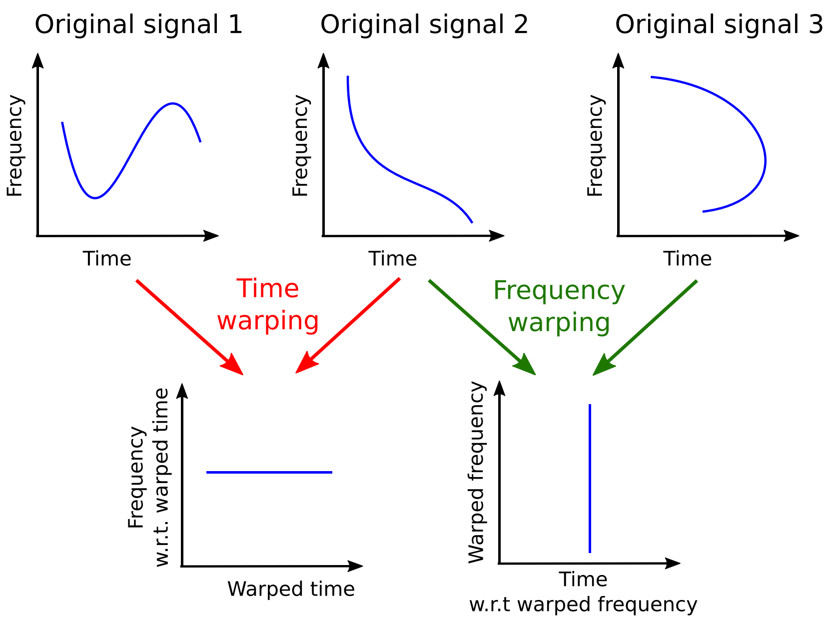

FIG. 1. (Color online) Diagram of the warping principles. Signal 1 must be warped using time-warping. Signal 3 must be warped using frequency-warping. Signal 2 can be warped using either time-warping of frequency warping.

A. Warping based on an ideal isovelocity waveguide model

The simplest waveguide model is the "ideal" isovelocity waveguide, with an isovelocity water column between a pressure release upper boundary and a rigid bottom. In such a waveguide, if the sound speed is c, the range is r, and the time origin is such that $t_s = 0$, then the modal phase in the time domain is given by[33]

$$\phi_{m_{iso}}(t) = 2\pi f_m \sqrt{t^2 - t_r^2}, \quad t > t_r, \tag{7}$$

with f_m the cutoff frequency of mode m and the receiver arrival time $t_r = r/c$. The corresponding warping function thus becomes

$$h_{iso}(t) = \sqrt{t^2 + t_r^2}, \tag{8}$$

and warping associated with $h_{iso}(t)$ will be defined as "isovelocity warping" in the following text. Since $h_{iso}(t)$ is independent of mode number, every mode can be warped at once with just a single transformation. Note that in general, $t_s \neq 0$ and the time origin of the analyzed signal must be manually adjusted. It is also important to note that Eq. (7) is valid only for $t > t_r$ (because the acoustic energy cannot travel faster than the sound speed c). As a result, the origin of the time axis becomes an important factor in practical analysis, a topic addressed in detail below.

Other environmental approximations also allow warping every mode simultaneously. These approximations include the approximated Pekeris waveguide,[13] the waveguide invariant[26,27] or beam-displacement ray-mode theory.[28] All these transforms are based on relatively simple environmental models that permit a closed-form expression for the modal phases ϕ_m, which leads to a closed-form expression of the warping function $h \propto \phi_m^{-1}$. They all have similar properties, and thus will not be presented in detail here.

B. Warping based on the exact dispersion of a single mode

Instead of using approximate closed-form expressions for ϕ_m, an alternative is to use numerical simulations, as can be obtained through a modal code such as KRAKEN[34] or ORCA.[35] The corresponding warping function can be numerically derived. In general, this approach creates a warping function h_m that depends on mode number. This numerical approach, dubbed "environment-specific warping" here, has been developed for ultrasonic guided wave studies,[29,30] but has never been previously applied to underwater acoustics.

In the underwater acoustic context, a valid question is whether environment-specific warping should be defined in the time or frequency domain. As modal propagation is described naturally in the frequency domain via Eq. (1), it is natural to consider frequency warping. Such a choice is reinforced by looking at Fig. 3(b), which presents a typical received signal in shallow water and its associated dispersion curves. At a given instant, a given mode may exist at several frequencies (e.g., at $t = 0.7$ s, subplot b shows mode 2 exists at $f = 28$ Hz and at $f = 103$ Hz). Mathematically speaking, the mode's instantaneous frequency (i.e., the evolution of its frequency with respect to time) is non-injective, and therefore no time-warping exists for making mode 2 a continuous tone. However, for a given frequency, every mode exists at only one time, and so the mode group delay (i.e., the evolution of its time of arrival with respect to frequency) is injective. Environment-specific warping must therefore be performed in the frequency domain.

If a numerical solution of the wave number $\widehat{k_m(f)}$ is available, then the warping function becomes

$$h_m(f) \propto \left(r\widehat{k_m(f)} - 2\pi j f t_s\right)^{-1}. \tag{9}$$

The function $h_m(f)$ depends on range r and on the source emission time t_s. If the latter quantity is known (or can be estimated from the data), then the time origin can be translated so that $t_s = 0$ (as is routinely done for isovelocity warping). In this case, Eq. (9) simplifies into

$$h_m^{t-trans}(f) \propto \widehat{k_m(f)}^{-1} \tag{10}$$

and becomes independent of the source range r.

Setting $t_s = 0$ is appealing in principle, as the resulting environment-specific warping operation becomes insensitive to range. However, the received signal time series will consist of a long noise period without acoustic energy (from $t = 0$ to $t = r/v_{g_{max}}$) followed by a short interesting period with acoustic energy (from $t = r/v_{g_{max}}$ to $t = r/v_{g_{min}}$), with $v_{g_{min}}$ and $v_{g_{max}}$ being the maximal and minimal group velocity. As we are dealing with the signal in the frequency domain, the samples associated with times before the signal's arrival cannot simply be discarded (as is routinely done for isovelocity warping). As a result, most of the computational cost associated with environment-specific warping would be used to warp noise. A practical implementation of environment-specific warping is facilitated by setting a negative t_s, such that the time origin is slightly before $t = r/v_{g_{max}}$. This drastically reduces the noise period without acoustic energy, which now lies from $t = 0$ to $t = r/v_{g_{max}} + t_s$ (with $t_s < 0$). As a result, the computational burden can be greatly decreased, at the cost of making the environment-specific sensitive to range, since $t_s \neq 0$. Note also that whatever t_s, it is possible to compute warping using fast operators.[36]

C. Phase compensation

Environment-specific warping transforms a broadband modal arrival into a Dirac function in the time domain. This goal can be reached with another method defined here as "phase compensation." If $\widehat{k_m(f)}$ is available, one can simply compensate the phase of the frequency-domain received signal $y(f)$. This phase-compensated signal $y_{pc}(f)$ is defined as

$$y_{pc}(f) = y(f) e^{-jr\widehat{k_m(f)}}. \tag{11}$$

This approach has been used in the past for geoacoustic inversion.[37] It has also been used to define a dedispersion transform in Ref. 38 [except that $\widehat{k_m(f)}$ was approximated using the waveguide invariant]. Phase compensation is closely related conceptually to numerically backpropagating a mode m,[39,40] except that in phase compensation only the phase is backpropagated. Note how Eq. (11) indicates that phase compensation is insensitive to t_s, and thus to time origin, but is sensitive to range. Phase compensation is invertible; the original signal is recovered through $y(f) = y_{pc}(f) e^{jr\widehat{k_m(f)}}$.

IV. APPLICATION TO SIMULATED ARCTIC WAVEGUIDE

In this section, isovelocity warping, environment-specific warping and phase compensation are applied to simulated data, to assess their capacity to filter modes and reliably estimate their amplitudes.

A. Environment and simulation description

The considered environment is a typical shallow water Arctic waveguide in summer. The water column depth is $D = 51$ m, and it has a downward-refracting sound speed profile, as shown on Fig. 2. The seabed is layered. It consists in a sandy sediment layer (sound speed $c = 1650$ m/s, density $\rho = 1.5$, width $h = 20$ m, attenuation $\alpha = 0.1$ dB/λ) over a semi-infinite basement (sound speed $c_b = 2000$ m/s, density $\rho_b = 2$, attenuation $\alpha = 0.1$ dB/λ). The considered range is $r = 8$ km. Source and receiver depths are $z_s = z_r = 45$ m, which have been chosen so that the first few modes are evenly excited.

The modal wave numbers $\widehat{k_m(f)}$ and depth functions $\widehat{\Psi_m(f)}$ are numerically estimated using ORCA[35] for frequencies between $f_{\min} = 0$ Hz and $f_{\max} = 250$ Hz with frequency steps $\Delta f = 0.25$ Hz. They are combined using Eq. (1) to form the impulse response of the waveguide $y(f)$. The received signal $y(t)$ is obtained through an inverse Fourier transform of $y(f)$ (which is equivalent to considering a perfectly impulsive source with $f_{\max} = 250$ Hz and $t_s = 0$). The sampling frequency associated with $y(t)$ is $F_s = 500$ Hz. Note that the simulation parameters (particularly r, $f_{\max}$ and Δf) have been carefully chosen to prevent time-aliasing (i.e., respecting Nyquist-Shannon theorem when computing $y(t)$ with the inverse Fourier transform) while at the same time minimizing the required number of samples.

The spectrogram of the simulated signal is presented in Fig. 3(a), while Fig. 3(b) shows the theoretical dispersion curves of the first five modes. It is interesting to note that modes 1 and 2 intersect around 180 Hz, a situation that can be explained by the water sound speed profile. Below 100 Hz, mode 1 is free: it has a sinusoidal behavior over the whole water column, and its boundaries are defined by reflection from the ocean surface and bottom. But above 200 Hz, mode 1 becomes trapped in the deeper portion of the water column: it has an exponential behavior for shallow depths, and its upper boundary is defined by in-column refraction. As a result the effective group velocity of mode 1 drops (as the bulk of the mode is in the slowest part of the water column), and the arrival time of mode 1 begins to increase with increasing frequency, eventually crossing that

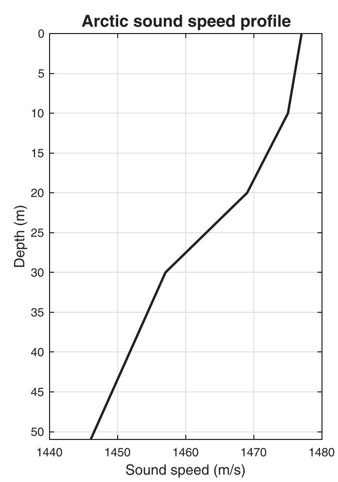

FIG. 2. Arctic sound speed profile, as used for simulations.

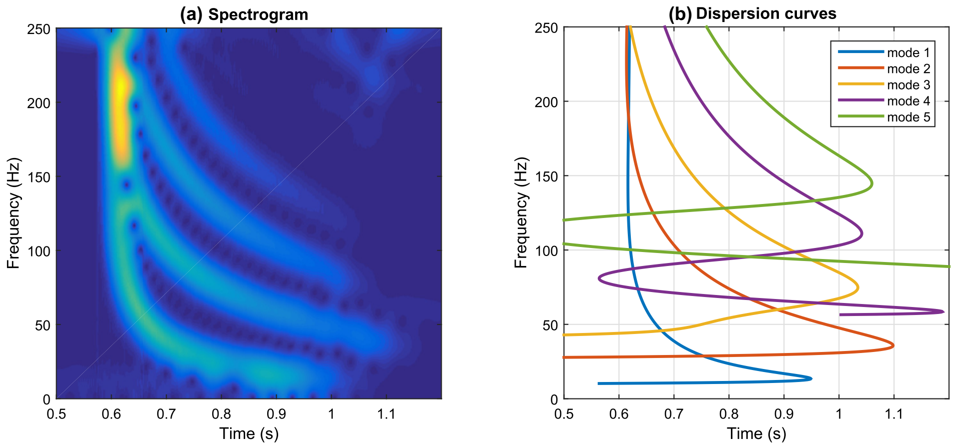

FIG. 3. (Color online) (a) Spectrogram of the simulated signal (arbitrary linear color scale) and (b) theoretical dispersion curves of the first five modes.

of mode 2, which remains untrapped. This intersection obviously provides difficulties for subsequent modal filtering. Moreover, for each mode, a similar phenomenon occurs between the Airy phase and cutoff frequency, when the mode begins to be trapped in the seabed. In this frequency band the modal dispersion curve makes a turnaround in the TF domain (e.g., between 27 and 35 Hz for mode 2). Such physics are not incorporated into the isovelocity warping function.

B. Single receiver illustration

Here the simulated signal presented in Fig. 3(a) is transformed using isovelocity warping, environment-specific warping and phase compensation.

1. Isovelocity warping

Because the signal has been simulated into a realistic waveguide, isovelocity warping must be used with care. In particular, one must choose t_r and define the signal's time origin. This is usually performed as follows:

(1) Select the signal sample that corresponds to the earliest high-frequency arrival, denoting this sample as t_{start}.
(2) Define t_r using any available environmental information.
(3) Assume that source emission time is $t_s = t_{\mathrm{start}} - t_r$ and shift the time axis so that $t_s = 0$.

This procedure is robust to mismatches in t_r, as long as t_{start} is correctly chosen. As a result, isovelocity warping has been successfully applied in many scenarios where t_r was completely unknown (e.g., passive source localization with unknown r[19–21]).

Figure 4 plots the Artic time-domain signal using two different t_{start} values, with the time axis defined so that $t_{\mathrm{start}} = 0$ to facilitate reading. In other words, the sample that corresponds to $t = 0$ in Fig. 4 is the sample that has been selected for step 1 in the isovelocity warping procedure. The "natural" t_{start} corresponds to the earliest high-frequency modal arrival. In this case, it corresponds to the mode 2 arrival at 250 Hz [see Fig. 3(b)]. Another "early" t_{start}, defined 30 ms earlier that the natural t_{start}, is also analyzed, for reasons that will become clear shortly.

Figure 5 shows the spectrogram of these signals after isovelocity warping. None of the modes are strictly tonal; a logical result, as isovelocity warping is based on a simplistic model that differs from the Arctic environment. The mode separation decreases at low warped times. In the original (non-warped) domain, this corresponds to early times where all the modes are merging at higher frequencies. The most interesting feature of Fig. 5 is probably the crossing between mode 1 and 2 at early warped time, which obviously corresponds to the crossing between mode 1 and 2 in the original domain.

2. Environment-specific warping and phase compensation

Figure 6 shows the results of environment-specific warping and phase compensation when $\widehat{k_1(f)}$ is used for the transformations. Figure 7 shows the results of environment-specific warping and phase compensation when $\widehat{k_2(f)}$ is used for the transformations. Because the model that is used for environment-specific warping and phase compensation is the same as that used to generate the

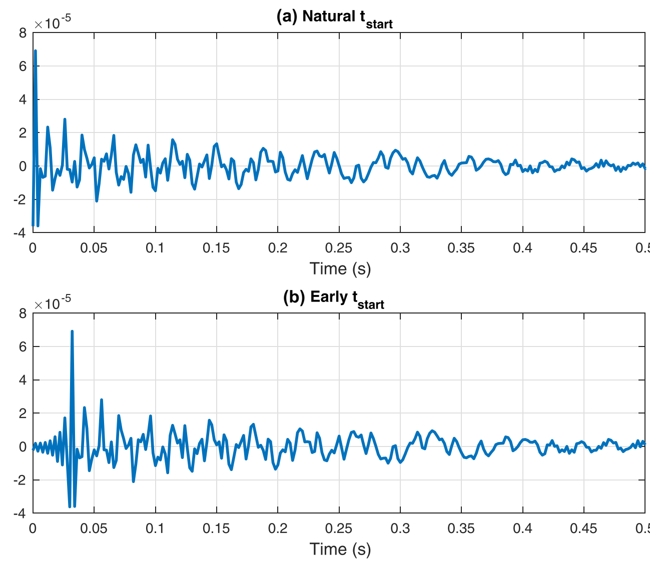

FIG. 4. (Color online) Time domain signal for two different values of t_{start}: (a) Natural t_{start} and (b) Early t_{start}. Note how the time axis has been adjusted so that $t_{\mathrm{start}} = 0$ on each plot in order to facilitate reading.

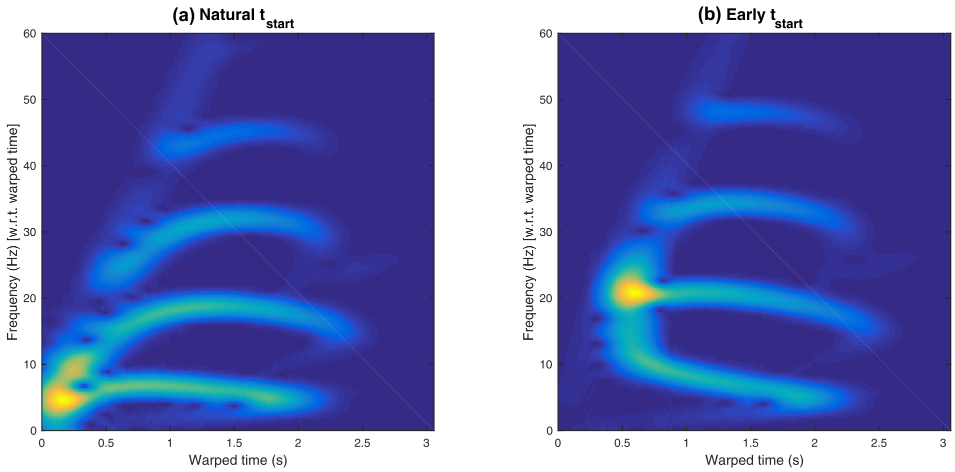

FIG. 5. (Color online) Spectrogram of the simulated signal after isovelocity warping (arbitrary linear color scale). Warping has been computed using (a) Natural t_{start} and (b) Early t_{start}.

simulations, modes 1 and 2 become perfect impulses in Figs. 6 and 7. Environment-specific warping and phase compensation yield the same results here. Note that whatever the transform used, it remains impossible to perfectly separate modes 1 and 2, since they cross each other in the physical TF domain. However, the transformed mode is always strictly vertical, even at low frequencies, and both methods successfully take into account the modal turn-around at the Airy phase.

C. Mode amplitude estimation using a single receiver

Mode filtering of the simulated signal is performed on a single receiver using the method presented in Ref. 14. First, the received signal is transformed, using either isovelocity warping, environment-specific warping or phase compensation. Regardless of the method used, the transformed result is defined here as the warped signal. The spectrogram of this warped signal is computed and used to design a TF filter to isolate a given (warped) mode. The filtered mode (in the original domain) is then obtained through inverse warping (or inverse phase compensation).

Figure 8 presents mode-filtered results for modes 1 and 2. One immediately notes that all methods fail to filter the modes for frequencies higher than 150 Hz. At these frequencies modes 1 and 2 merge, and no method is able to separate them. Environment-specific warping and phase compensation have similar results; they allow a good recovery of modes 1 and 2 across a broad bandwidth. Isovelocity warping allows a good recovery of mode 2, with slightly better performances than environment-specific warping and/or phase compensation. This can be explained by the fact that isovelocity warping theoretically separates every mode at once, and thus maximizes the modal separation. However, filtering mode 1 with isovelocity warping highly depends on the value chosen for t_{start}. With an early t_{start}, mode 1 recovery is excellent. However, with the natural t_{start}, the filtering performance decreases, and the filtered mode 1 amplitude oscillates with frequency. This phenomenon could have been predicted by looking at the warped spectrogram on Fig. 5. The separation between (warped) modes 1 and 2 is better with an early t_{start}. More specifically, warped modes 1 and 2 merge together more slowly with a natural t_{start}, while their intersection is perpendicular with an early t_{start}. This last case (perpendicular intersection) is obviously the best to separate two interfering TF structures. This early t_{start} was actually selected (via trial-and-error) to obtain such a result. However, note how this choice t_{start} is not optimal for the whole signal, as modes 2 and 3 now interfere together (Fig. 5).

Overall, the filtering performance depends strongly on the specific design of the TF filter (accomplished manually in this study), so that a true performance comparison is beyond the scope of this paper. Nonetheless, we do note that the TF filter design is relatively easy for environment-specific warping and/or phase compensation, since the

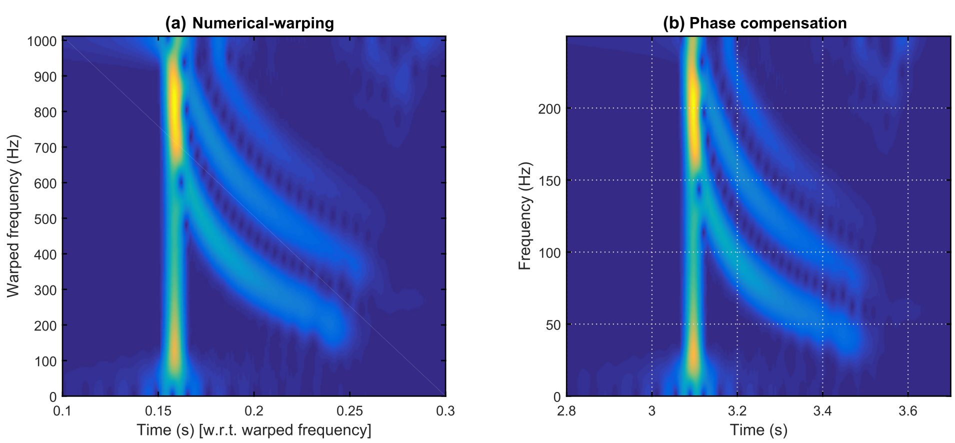

FIG. 6. (Color online) Spectrograms of the simulated signal after (a) environment-specific warping and (b) phase compensation (arbitrary linear color scale). The two transformations are performed for mode 1.

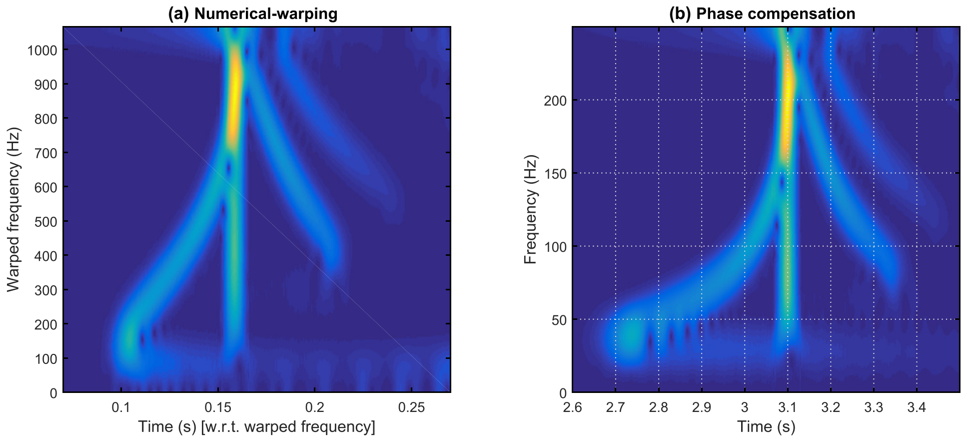

FIG. 7. (Color online) Spectrograms of the simulated signal after (a) environment-specific warping and (b) phase compensation (arbitrary linear color scales). The two transformations are performed for mode 2.

warped mode becomes a perfect impulse. However, because multiple modes are present, the selection of a time window implies collecting energy from other modes, so that perfect filtering is impossible. By contrast the design of the TF filter for isovelocity warping can often be tedious, requiring a trial and error iteration over t_{start}, a procedure that sometimes must be repeated for different modes. Since the model used by isovelocity warping gives up certain mode portions (e.g., Airy phase), perfect filtering is also impossible.

D. Mode amplitude estimation along a vertical line array

The previous simulation is completed by simulating a VLA of receivers. The VLA consists of ten hydrophones, from $z_1 = 5$ m to $z_{10} = 50$ m with a $\Delta z = 5$ m spacing. As proposed in Ref. 14, mode amplitude is estimated on each receiver independently. The objective here is to illustrate the filtering capacities of the various warping and phase compensation methods.

1. Isovelocity warping

Figure 9 presents the mode amplitude estimation at $f = 80$ Hz obtained with isovelocity warping, with other frequencies displaying similar results. A choice of an early t_{start} allows excellent recovery of each mode. In contrast the natural t_{start} recovers modes 2 and 3, but introduces errors into mode 1.

This simulation reproduces a phenomenon that has been observed by multiple researchers: that estimating the first mode amplitude is sometimes problematic (e.g., see Fig. 9 in Ref. 14 or Fig. 8 in Ref. 23). The simulation also identifies the cause: the difficulty in correctly estimating t_{start} for experimental data collected in an unknown environment. Recovering the first mode from a complex environment seems to require an early t_{start}, while other modes are better recovered with a later t_{start} (as a reminder, modes 2 and 3 interfere together when using an early t_{start}, see Fig. 5). Until now, most researchers using warping have used a single t_{start} to recover every mode, thus leading to a poor estimation of mode 1. Such phenomenon also impacts the mode dispersion curve estimation. As examples, one can examine Fig. 3(a) in Ref. 14, Fig. 4(a) in Ref. 18 and/or Fig. 3 in Ref. 41. In all these cases, the estimated dispersion curve of mode 1 mismatches the underlying spectrogram, while other modes recover their correct dispersion.

Figure 8 also dramatically illustrates how the natural t_{start} choice generates a poorly estimated mode 1 that highly oscillates with frequency. Indeed, the large errors for mode 1 in that figure makes one wonder how reasonable mode 1 depth functions are even possible. And yet, Fig. 9 reveals

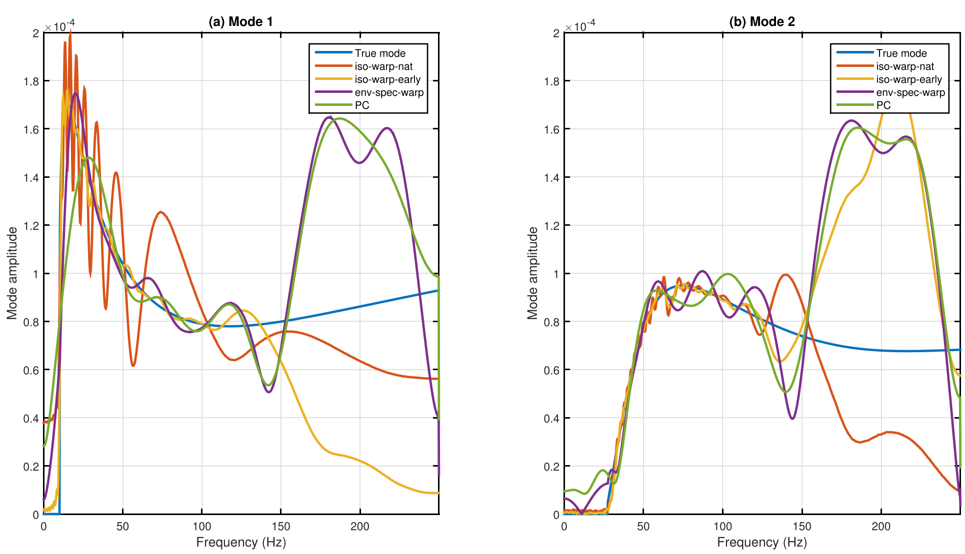

FIG. 8. (Color online) Mode-filtered results using isovelocity warping with natural t_{start} (iso-warp-nat), isovelocity warping with early t_{start} (iso-warp-early), environment-specific warping (env-spec-warp) and phase compensation (PC).

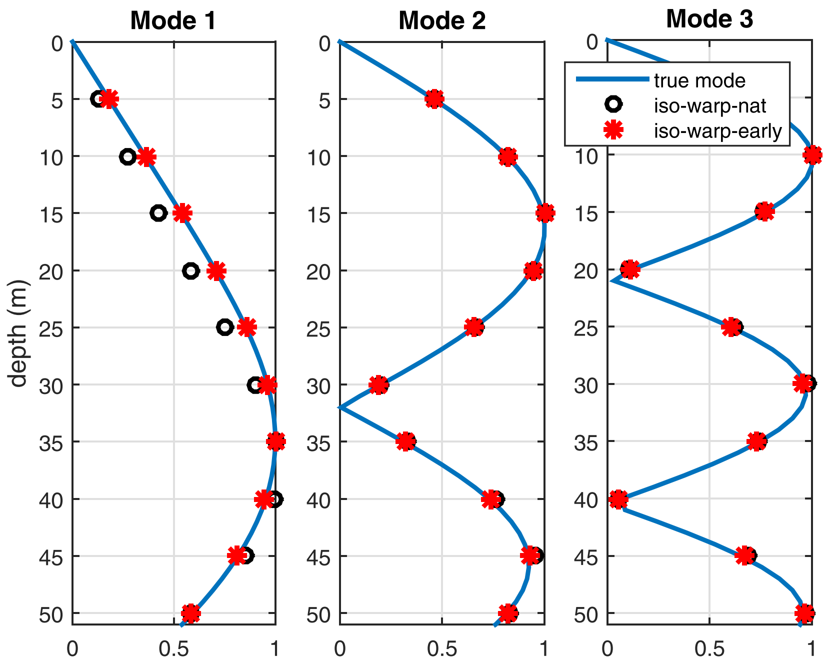

FIG. 9. (Color online) Mode amplitude estimation at 80 Hz along a VLA using isovelocity warping with natural t_{start} (iso-warp-nat) and with early t_{start} (iso-warp-early). The continuous curves represent the theoretical mode amplitudes over the whole water column. Mode amplitude has been normalized to facilitate reading (the maximal amplitude is 1).

that the same value of natural t_{start} still permits a relatively decent modal depth function to be extracted at a fixed frequency. Figure 10 explains this apparent contradiction by plotting the mode amplitude vs frequency for multiple receiver depth. The frequency oscillations created by modal interferences are highly correlated between receivers: the frequencies of dips and peaks barely change with depth. Put another way, the relative amplitudes of a mode at two different depths are only weakly dependent on frequency. Thus once mode depth functions are normalized per usual conventions, the impact of a poor choice of t_{start} on the modal depth function estimation is relatively limited. Applications that relay primarily on modal phase (e.g., source ranging) are barely affected by this phenomenon. However, the mismatch between warped and underlying mode shape can become important for source depth estimation and other applications that require precise mode amplitude estimates.

2. Environment-specific warping and phase compensation

Figure 11 presents the filtering results at $f = 80$ Hz for modes 1, 2, and 3. The performance of phase compensation and environment-specific warping are roughly the same. The small differences between the two methods are mainly due to the design of the TF filter (which was adjusted manually). Mode 1 is well-estimated with both methods, and similar results are obtained at other frequencies.

V. APPLICATION TO SHALLOW WATER 2006 EXPERIMENTAL DATA

If the time origin and source range are known, phase compensation and environment-specific warping have similar performances. As a reminder, phase compensation is insensitive to time origin, while environment-specific

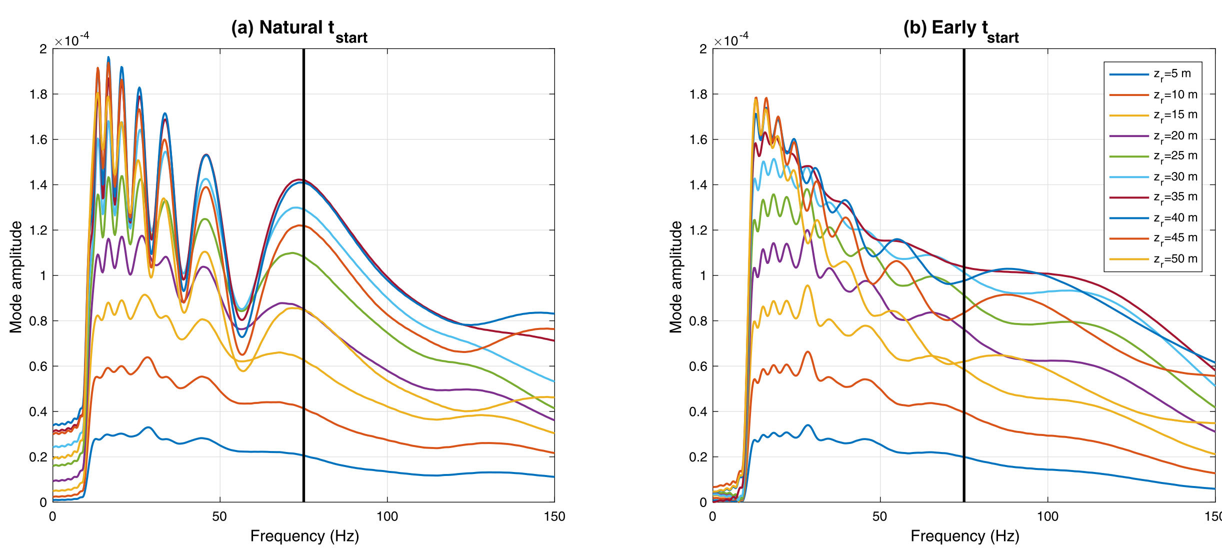

FIG. 10. (Color online) Mode 1 amplitude, as estimated over the VLA using isovelocity warping with (a) natural t_{start} and (b) early t_{start}. The vertical bar is set at 80 Hz, which is the frequency that has been used to estimate modal depth function in Fig. 9.

warping is insensitive to range. In the following, we will focus on an experimental data recorded during the Shallow Water 2006 (SW06) experiment, where the range is known and time origin unknown. As a result, we will focus on phase compensation vs isovelocity warping results.

A. Data description

In summer 2006 the SW06 experiment was conducted on the New Jersey continental shelf.[42] One objective of this experiment was to characterize the seabed in a complex oceanic environment within the 50–20 000 Hz frequency band. On August 31, light bulbs were deployed as low-frequency impulsive sources: their spectrum is roughly flat over the 30–200 Hz band. A single light bulb implosion is used as the source for this paper. The source position was (39°04.72′N, 72°59.86′W) and its depth was $z_s \simeq 22$ m. The acoustic field was collected on MPL-VLA1 located around (39°01.44′N, 73°02.39′W). It consists of 16 hydrophones and it spans the water column from $z_1 = 18.3$ m to $z_{16} = 78.8$ m with a $\Delta z = 3.75$ m spacing. The recording sampling frequency is 5000 Hz, but the data were subsampled by a factor of 8 before analysis (which leads to a sampling frequency of 625 Hz). The source/receiver range is $r \simeq 7$ km. This distance is relatively short for such a low-frequency configuration so that the modes are not naturally separated on the received signal. The track was chosen to be as range-independent as possible, and the water depth is $D = 79$ m.

The event analyzed here was also analyzed in Ref. 15. During the light bulb experiment, the water column was monitored using a conductivity-temperature-depth probe (CTD41). The seabed structure and geoacoustic parameters were previously estimated in Ref. 15 using Bayesian inversion methods. Over the frequency band of interest the seabed is modeled as a single layer over a basement. The maximum *a posteriori* estimate of the seabed parameters are as follows: layer sound speed $c_p = 1604$ m/s, layer density $\rho = 1.8$ g/cm^3, layer width $h = 25$ m, basement sound speed $c_b = 2132$ m/s and basement density $\rho_b = 1.48$ g/cm^3. Here, a constant attenuation of 0.01 dB/λ is assumed for the seabed. This environmental information is used here to estimate the experimental wave number $\widehat{k_m(f)}$, and is also used as ground truth to benchmark the estimated mode amplitudes. However, one should recall that the *a posteriori* estimate of the seabed parameters that are used here are not an actual ground truth, and that a mismatch between $\widehat{k_m(f)}$ and the true $k_m(f)$ cannot be avoided.

B. Single receiver illustration

The analysis focuses first on the deepest hydrophone, where the modes are evenly excited. Figure 12(a) shows the spectrogram of the received signal, while Fig. 12(b) shows the isovelocity warping result. On each subfigure, the modes are labeled to ease the reading. The warped modes are obviously not continuous tones, as the isovelocity model does not match the experimental environment. Also, note that Fig. 12 is computed with what we believe to be the "natural" t_{start}. One can note how the beginning of mode 1 is slightly clipped on the received spectrogram. However, the chosen t_{start} is good enough so that mode 2, 3, and 4 are clearly separated.

Phase compensation is also applied on the received signal. It has been performed for modes 1, 2, 3, and 4 (using the corresponding $\widehat{k_m(f)}$), and the spectrogram of the result is presented on Fig. 13. The modes have been labeled on each subfigure whenever it is possible, to identify them. One would expect that when $\widehat{k_{m_0}(f)}$ is used for phase compensation, the spectrogram of the result would show mode m_0 has a perfect impulse, but this is not the case. None of the targeted modes (shown by a red arrow on Fig. 13) are perfect impulses, an indication that the environmental model used for phase compensation is slightly mismatched. This conclusion is both interesting and surprising. On the one hand, it shows that phase compensation is an easy method to verify

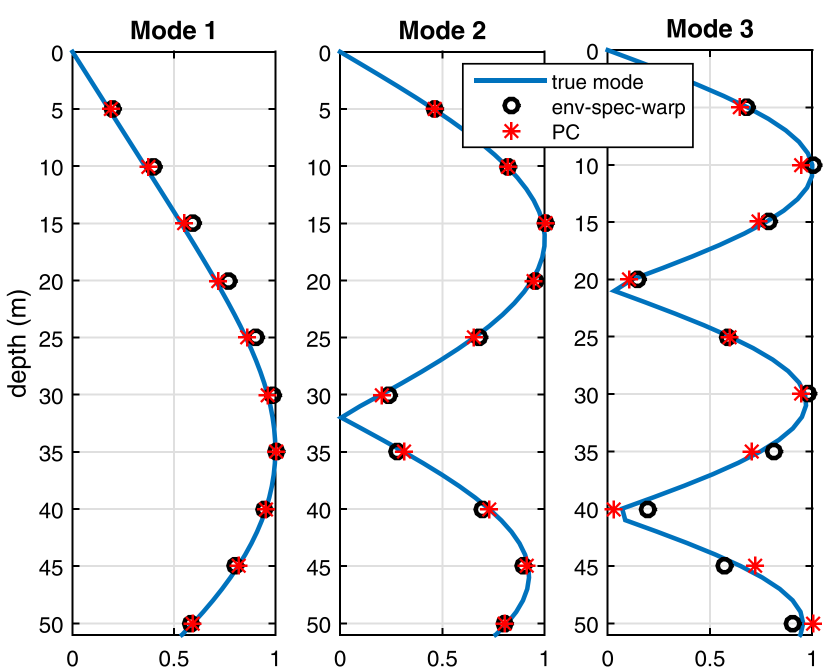

FIG. 11. (Color online) Mode amplitude estimation at 80 Hz along a VLA using environment-specific warping and phase compensation. The continuous curves represent the theoretical mode amplitudes over the whole water column. Mode amplitude has been normalized to facilitate reading (the maximal amplitude is 1).

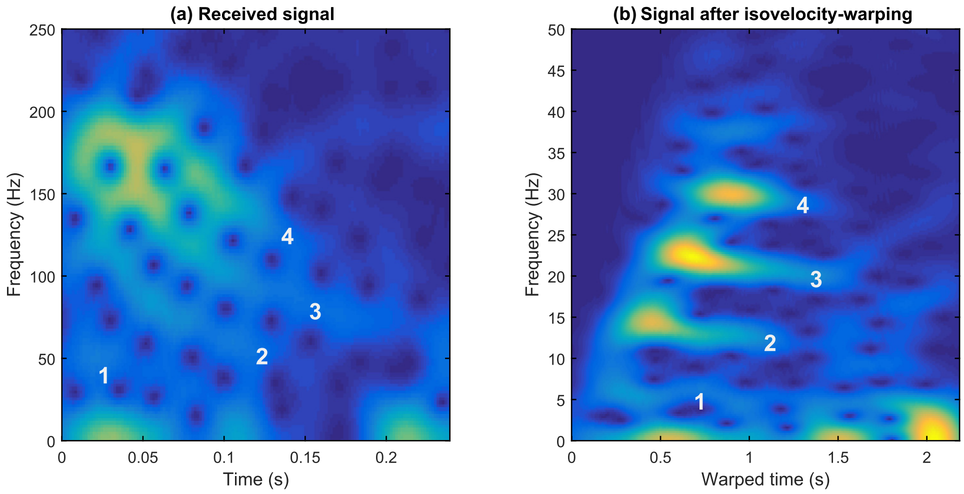

FIG. 12. (Color online) (a) Spectrogram of the received signal and (b) spectrogram of the signal after isovelocity warping (arbitrary linear color scales).

the accuracy of an environmental model. On the other hand, it is a good reminder that uncertainties of the geoacoustic estimate cannot be blithely discarded. The maximum *a posteriori* estimate of the seabed parameters that are used here do not fully capture the seabed physics.

C. Mode amplitude estimation along a vertical line array

Mode amplitudes were also estimated on every receiver of the VLA, performed receiver by receiver using both isovelocity warping and phase compensation. Note that isovelocity warping is applied with the t_{start} that has been used to generate Fig. 12, except for mode 1, where an earlier t_{start} is applied.

Figure 14 presents the filtering results at $f = 150$ Hz for modes 1–4. The filtered modes are compared with simulated modal depth functions, which have been obtained using the best-estimated environmental parameters. Any quantitative comparison is impractical, as the underlying true depth functions are unknown. However, one notes that both isovelocity warping and phase compensation are consistent. The recovered mode 1 is not perfectly smooth, suggesting that its estimation could be improved further. Nonetheless, the mode 1 recovery is much improved over Ref. 14 or Ref. 23, emphasizing the fact that mode amplitude estimation can be improved by simply changing t_{start} (when isovelocity warping is used), or by using a transform based on an accurate environmental model (either phase compensation or environment-specific warping).

VI. CONCLUSION

In the past few years, the possibility of analyzing modal dispersion with a single receiver has been popularized in the ocean acoustic community. In such a single receiver context, it is natural to resort to TF analysis. However, at short ranges, the modes interfere and individual modal arrivals cannot be resolved using conventional TF analysis. Nonetheless, it is known that a non-linear sampling method called isovelocity warping allows modal filtering at relatively short ranges. The main characteristic of isovelocity warping is that it warps every mode simultaneously, and requires nearly no environmental knowledge. However, isovelocity warping requires defining an arbitrary time origin, which corresponds to the source emission time in an

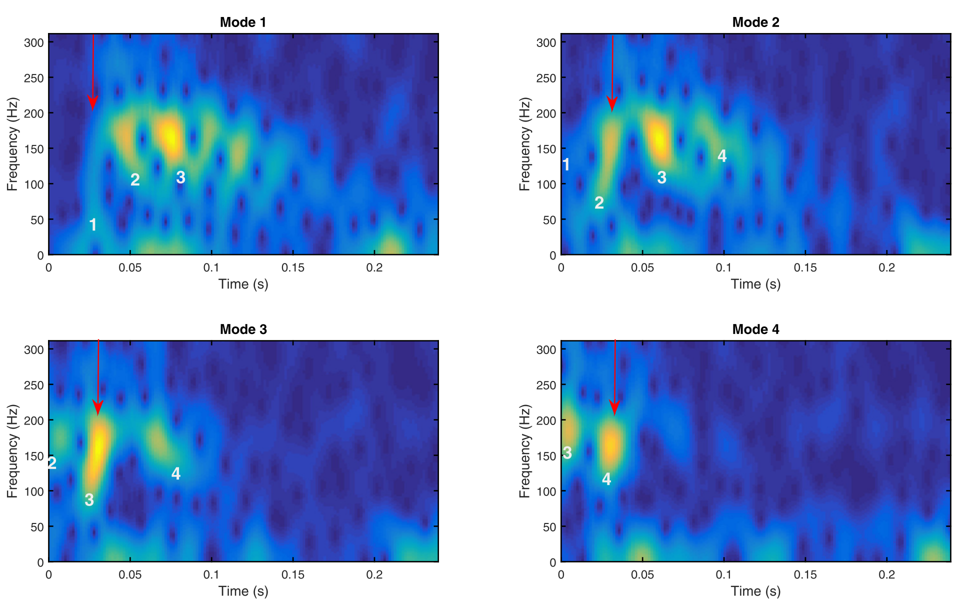

FIG. 13. (Color online) Spectrograms of the phase-compensated signals, with phase compensation performed for modes 1 to 4 (arbitrary linear color scales). On each subfigure, the vertical red arrow shows the mode that has been phase-compensated.

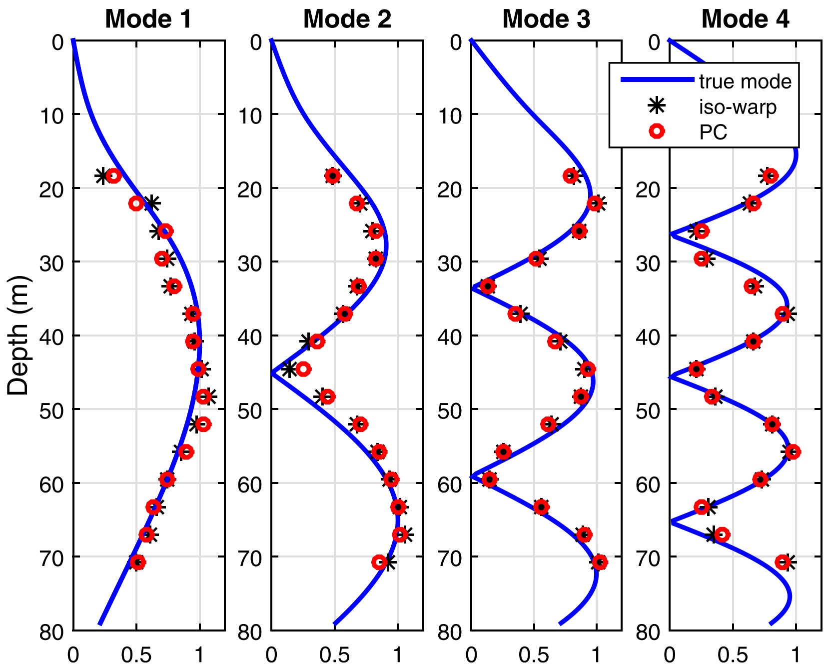

FIG. 14. (Color online) Mode amplitude at 150 Hz, estimated along the VLA on the SW06 data using isovelocity warping (asterisk) and phase compensation (circle). The continuous curves represent the theoretical mode amplitudes over the whole water column.

isovelocity waveguide, but has no physical definition in a more realistic environment.

This study has demonstrated the importance of selecting an appropriate time origin when recovering mode amplitudes, particularly for the first mode. Furthermore, this study shows that the appropriate time origin can change, depending on the mode chosen. Filtering the first mode arrival is particularly sensitive to this phenomenon, and mode 1 requires an earlier time origin than the other modes to allow accurate mode amplitude recovery.

This study has also presented alternative modal filtering methods based on another philosophy. The proposed environment-specific warping takes into account all the available environmental information, adapted for a given mode out of a set of modes. Thus, if the signal contains M modes, M different environment-specific warpings must be considered. Environment-specific warping is conceptually equivalent to phase compensation, a processing that is simpler and computationally lighter. It is interesting to remark that when two modes cross each other in the TF domain, they also cross after warping and/or phase compensation. Unfortunately, nothing can be done about it. The best thing to do in this case is to use the transform that minimizes the overlap between the crossing modes, and to avoid using the information for this frequency/modal band for inversion.

Isovelocity warping, environment-specific warping and phase compensation all extract the amplitudes, but isovelocity warping is the easiest transform to apply to modes 2 and higher. The fact that isovelocity warping transforms every mode at once is a major advantage, which greatly facilitates filtering. Environment-specific warping and phase compensation are the easiest transform to estimate the amplitude of mode 1. Indeed, mode 1 is the mode that is most affected by the water column, which is why taking into account such environmental information is important. However, mode 1 can also be filtered using isovelocity warping, as long as an adapted time origin is carefully chosen. Overall, if one pursues an accurate match with the physical phenomenon, it is better to work with environment-specific warping. However, if one wants to isolate only part of the modal spectrum, then it is simpler and faster to work with isovelocity warping.

A key result of this paper is that improved estimates of mode 1 amplitude are possible, regardless of the particular method chosen. Previous works employing isovelocity warping were unable to correctly resolve this mode, which may have biased subsequent applications (such as the estimation of sediment attenuation at low frequencies). Reliable estimates of mode 1 will substantially improve source localizations (in range and depth) using single receiver MMP in situations where only a few modes are detected. Another final result is that phase compensation provides an easy method to check the validity of an environmental model on real data.

The results obtained here can be directly transferred toward the bioacoustics community. Indeed, most passive acoustic monitoring systems consist of isolated hydrophones. As a result, they usually do not have the ability to estimate positions of the animals. The capacity to correctly filter modes with a single receiver in shallow water opens the door to single-receiver MMP, which in turns will allow revisiting bioacoustic dataset for localizing baleen whales. This, obviously, would be impossible using classical array-based processing such as MFP.

Future work should also consider geoacoustic inversion methods based on phase compensation and/or environment specific warping. Two options arise here. On the one hand, because they depend on a specific environment model, it is possible to include phase compensation or environment specific warping into the inversion scheme. On the other hand, it is possible to do sequential inversions, and gradually refine the model that is used to transform the signal. Accurate mode amplitude estimates are of paramount importance to infer the seabed attenuation at low frequencies, which is unknown in most sediment type at the considered low-frequencies.

ACKNOWLEDGMENTS

This work was supported by the North Pacific Research Board, Project 1416. This work is NPRB publication number 632. S.C.'s contribution was supported by the Engineering and Physical Sciences Research Council Grant number EP/J015180/1 and the MOD University Defence Research Collaboration in Signal Processing. The authors thank R. Chapman for helpful discussions.

[1]A. Baggeroer, W. Kuperman, and P. Mikhalevsky, "An overview of matched field methods in ocean acoustics," IEEE J. Oceanic Eng. **18**(4), 401–424 (1993).
[2]M. Snellen, D. Simons, M. Siderius, J. Sellschopp, and P. Nielsen, "An evaluation of the accuracy of shallow water matched field inversion results," J. Acoust. Soc. Am. **109**(2), 514–527 (2001).
[3]C. Huang, P. Gerstoft, and W. Hodgkiss, "Uncertainty analysis in matched-field geoacoustic inversions," J. Acoust. Soc. Am. **119**(1), 197–207 (2006).
[4]S. E. Dosso and J. Dettmer, "Bayesian matched-field geoacoustic inversion," Inv. Problems **27**, 055009 (2011).
[5]T. Yang, "Effectiveness of mode filtering: A comparison of matched-field and matched-mode processing," J. Acoust. Soc. Am. **87**(5), 2072–2084 (1990).
[6]T. Yang, "A method of range and depth estimation by modal decomposition," J. Acoust. Soc. Am. **82**, 1736–1745 (1987).
[7]F. Jensen, W. Kuperman, M. Porter, and H. Schmidt, *Computational Ocean Acoustics*, 2nd ed. (AIP, New York, 2011), Chap. 5, pp. 337–455.
[8]J. Buck, J. Preisig, and K. Wage, "A unified framework for mode filtering and the maximum a posteriori mode filter," J. Acoust. Soc. Am. **103**(4), 1813–1824 (1998).
[9]T. Neilsen and E. Westwood, "Extraction of acoustic normal mode depth functions using vertical line array data," J. Acoust. Soc. Am. **111**(2), 748–756 (2002).
[10]S. Jesus, M. Porter, Y. Stephan, X. Demoulin, O. Rodriquez, and E. Coelho, "Single hydrophone source localization," EEE J. Oceanic Eng. **25**(3), 337–346 (2000).
[11]J. P. Hermand, "Broad-band geoacoustic inversion in shallow water from waveguide impulse response measurements on a single hydrophone: Theory and experimental results," IEEE J. Oceanic Eng. **24**, 41–66 (1999).
[12]T. C. Yang, "Dispersion and ranging of transient signals in the Arctic Ocean," J. Acoust. Soc. Am. **76**, 262–273 (1984).
[13]G. Le Touzé, B. Nicolas, J. Mars, and J. Lacoume, "Matched representations and filters for guided waves," IEEE Trans. Signal Processing **57**(5), 1783–1795 (2009).
[14]J. Bonnel, C. Gervaise, P. Roux, B. Nicolas, and J. Mars, "Modal depth function estimation using time-frequency analysis," J. Acoust. Soc. Am. **130**, 61–71 (2011).
[15]J. Bonnel, S. Dosso, and R. Chapman, "Bayesian geoacoustic inversion of single hydrophone light bulb data using warping dispersion analysis," J. Acoust. Soc. Am. **134**, 120–130 (2013).
[16]P. Petrov, "A method for single-hydrophone geoacoustic inversion based on the modal group velocities estimation: Application to a waveguide with inhomogeneous bottom relief," in *Days on Diffraction* (IEEE, New York, 2014), pp. 186–191.
[17]L. Feng-Hua, Z. Bo, and G. Yong-Gang, "A method of measuring the *in situ* seafloor sound speed using two receivers with warping transformation," Chin. Phys. Lett. **31**(2), 1–4 (2014).
[18]M. S. Ballard, G. V. Frisk, and K. M. Becker, "Estimates of the temporal and spatial variability of ocean sound speed on the new jersey shelf," J. Acoust. Soc. Am. **135**(6), 3316–3326 (2014).
[19]J. Bonnel, A. Thode, S. Blackwell, K. Kim, and A. Macrander, "Range estimation of bowhead whale (balaena mysticetus) calls in the arctic using a single hydrophone," J. Acoust. Soc. Am. **136**(1), 145–155 (2014).
[20]J. L. Crance, C. L. Berchok, J. Bonnel, and A. M. Thode, "Northeasternmost record of a north pacific fin whale (balaenoptera physalus) in the Alaskan chukchi sea," Polar Biol. **38**, 1767–1773 (2015).
[21]G. A. Warner, S. E. Dosso, D. E. Hannay, and J. Dettmer, "Bowhead whale localization using asynchronous hydrophones in the chukchi sea," J. Acoust. Soc. Am. **140**(1), 20–34 (2016).
[22]J. Zeng, N. R. Chapman, and J. Bonnel, "Inversion of seabed attenuation using time-warping of close range data," J. Acoust. Soc. Am. **134**, EL394–EL399 (2013).
[23]R. Duan, N. R. Chapman, K. Yang, and Y. Ma, "Sequential inversion of modal data for sound attenuation in sediment at the New Jersey Shelf," J. Acoust. Soc. Am. **139**(1), 70–84 (2016).
[24]B. Nicolas, G. Le Touzé, C. Soares, S. Jesus, and J. I. Mars, "Incoherent versus coherent matched mode processing for shallow water source localisation using a single hydrophone," Instrument. Viewpoint, **8**, 67–68 (2010).
[25]J. Bonnel and A. Thode, "Range and depth estimation of bowhead whale calls in the arctic using a single hydrophone," in *IEEE Sensor Systems for a Changing Ocean (SSCO)*, (2014), pp. 1–4.
[26]J. Bonnel, G. Le Touzé, B. Nicolas, and J. Mars, "Physics-based time-frequency representations for underwater acoustics: Power class utilization with waveguide-invariant approximation," IEEE Signal Processing Mag. **30**(6), 120–129 (2013).
[27]Y. B. Qi, S. H. Zhou, R. H. Zhang, and Y. Ren, "A waveguide-invariant-based warping operator and its application to passive source range estimation," J. Comput. Acoust. **23**, 1550003 (2015).
[28]H. Niu, R. Zhang, and Z. Li, "Theoretical analysis of warping operators for non-ideal shallow water waveguides," J. Acoust. Soc. Am. **136**(1), 53–65 (2014).
[29]L. De Marchi, A. Marzani, S. Caporale, and N. Speciale, "Ultrasonic guided-waves characterization with warped frequency transforms," IEEE Trans. Ultrason. Ferroelectr. Frequency Control **56**(10), 2232–2240 (2009).
[30]L. De Marchi, M. Ruzzene, B. Xu, E. Baravelli, and N. Speciale, "Warped basis pursuit for damage detection using lamb waves," IEEE Trans. Ultrason. Ferroelectr. Frequency Control **57**(12), 2734–2741 (2010).
[31]K. Xu, D. Ta, P. Moilanen, and W. Wang, "Mode separation of lamb waves based on dispersion compensation method," J. Acoust. Soc. Am. **131**(4), 2714–2722 (2012).
[32]R. Baraniuk and D. Jones, "Unitary equivalence: A new twist on signal processing," IEEE Trans. Signal Processing **43**(10), 2269–2282 (1995).
[33]I. Tolstoy and C. Clay, *Ocean Acoustics: Theory and Experiment in Underwater Sound* (Acoustical Society of America, New York, 1987).
[34]M. B. Porter, "The kraken normal mode program," Tech. Rep., DTIC Document, 1992.
[35]E. K. Westwood, C. Tindle, and N. Chapman, "A normal mode model for acousto-elastic ocean environments," J. Acoust. Soc. Am. **100**(6), 3631–3645 (1996).
[36]S. Caporale, L. De Marchi, and N. Speciale, "Fast computation of frequency warping transforms," IEEE Trans. Signal Processing **58**(3), 1110–1121 (2010).
[37]J. Bonnel, C. Gervaise, B. Nicolas, and J. Mars, "Single-receiver geoacoustic inversion using modal reversal," J. Acoust. Soc. Am. **131**(1), 119–128 (2012).
[38]D. Gao, N. Wang, and H. Wang, "A dedispersion transform for sound propagation in shallow water waveguide," J. Comput. Acoust. **18**(3), 245–257 (2010).
[39]C. Park, W. Seong, P. Gerstoft, and W. Hodgkiss, "Geoacoustic inversion using backpropagation," IEEE J. Oceanic Eng. **35**(4), 722–731 (2010).
[40]Y.-T. Lin, A. Newhall, and J. Lynch, "Low-frequency broadband sound source localization using an adaptive normal mode back-propagation approach in a shallow-water ocean," J. Acoust. Soc. Am. **131**, 1798–1813 (2012).
[41]P. Petrov, "A method for single-hydrophone geoacoustic inversion based on the modal group velocities estimation: Application to a waveguide with inhomogeneous bottom relief," in *IEEE Days on Diffraction* (2014), pp. 186–191.
[42]D. Tang, J. Moum, J. Lynch, P. Abbot, R. Chapman, P. Dahl, T. Duda, G. Gawarkiewicz, S. Glenn, J. Goff, H. Graber, J. Kemp, A. Maffei, J. Nash, and A. Newhall, "Shallow Water 06: A joint acoustic propagation/nonlinear internal wave physics experiment," Oceanography **20**, 156–167 (2007).